Scientia Iranica A (2018) 25(1), 33–49

SCIENTIA IRANICA

Sharif University of Technology
**Scientia Iranica**
*Transactions A: Civil Engineering*
http://scientiairanica.sharif.edu

# Determination of target time for endurance time method at different seismic hazard levels

**A. Bazmooneh*** **and H.E. Estekanchi**

*Department of Civil Engineering, Sharif University of Technology, Tehran, Iran.*

Received 12 May 2015; received in revised form 16 July 2016; accepted 19 November 2016

**KEYWORDS**
Performance-based design;
Endurance time method;
Risk assessment;
Seismic parameters;
Earthquake accelerograms.

**Abstract.** Various durations of Endurance Time Acceleration Functions (ETAFs) associated with different seismic hazard levels are presented to enable Endurance Time (ET) method for use in probabilistic seismic demand assessment studies. Various Intensity Measures (IMs) were, first, considered for establishing multiple "IM-duration" relationships. A set of 30 RC moment resisting frames were, then, subjected to IDA analysis using 44 ground motion records and the median IM values corresponding to different structural response levels were extracted. These values were compared with the ET-derived IMs by computing the errors corresponding to various demand levels and summating these errors over a complete range of response levels to derive an overall error index. The error indices were then averaged over all structural models and were compared for different IMs, revealing that maximum compatibility with the ETAF generation method dominated selection of the best IM.



## 1. Introduction

"Endurance Time" (ET) method is a progressive dynamic analysis, which determines seismic performance of structures under sequentially increasing predetermined acceleration functions (Figure 1) [1]. This method tries to assess seismic performance of structures under earthquakes with various intensities and seismic hazard return periods, but with considerably lower analysis costs. This method can be extensively utilized for seismic assessment and performance-based design and optimization of structures [2]. For instance, according to the classical time-history analysis, seven records will be required for each seismic hazard level [3]; thus, if four seismic hazard levels are to be considered, 28 time-history analyses have to be done. However, by utilizing ET method, the number of required analyses is reduced to three. It must also be noted that using seven ground motion records will not be able to fully cover the uncertainties associated with earthquake and a precise evaluation will need employment of more records. The analysis cost inherent to an accurate assessment performed with conventional ground motion records will, therefore, be more pronounced and the advantage of using ET method will be more elaborated.

In this method, after exerting a proper Endurance Time Acceleration Function (ETAF) to the structure, the specific time of the structural analysis at which the desired performance criteria (e.g., allowable drift or allowable rotation of beams) are violated is the "endurance time" of that structure. It is noteworthy that different damage indices can also be candidates for reflecting the limit states of the structure [4,5].

The ETAFs have been designed in such a way that for a base target time, their response spectrum matches

*. *Corresponding author.*
*E-mail addresses: a.bazmooneh@gmail.com (A. Bazmooneh); stkanchi@sharif.edu (H.E. Estekanchi)*

doi: 10.24200/sci.2017.4176

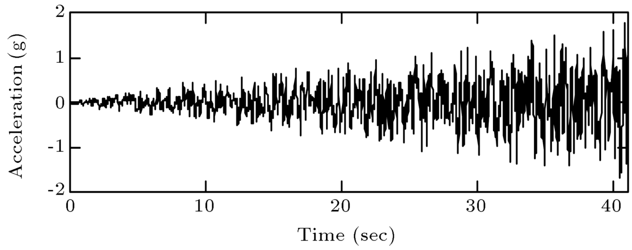


**Figure 1.** A typical "endurance time" acceleration function.

a target spectrum (the base spectrum for generating the "endurance time" acceleration functions). Being derived so, multiplying the duration time (base target time) by an "A" factor also leads the target spectrum to be amplified by "A" [6] (Figure 2). In other words, the response of structures subjected to different durations of the ETAFs spells structural demands corresponding to different seismic hazard levels.

The aim of this article is to determine the seismic hazard level corresponding to various "endurance time" values. Having established this correspondence, ET method can be used for evaluating seismic performance of structures at hazard levels expressed in terms of intensity parameters commonly employed by seismic standards. Using the probabilities associated with different intensity levels, a correspondence can be established between the endurance time and the return period of earthquakes. Equipping the ET method with this mapping will also make it an efficient candidate for performance-based design of structures.

To attain the purpose of this article, three ETAFs, generated previously (see [6]) using the average spectrum of seven ground motion records, were considered. The difference in the acceleration history of the so-called "e", "f", and "h" ETAFs was assumed to represent, to some extent, the record-to-record variability of ground motions. The seven records used in generating these ETAFs were selected according to FEMA 440 [7] suggestion. For extracting the endurance time equivalent to a specific seismic hazard level, the ETAF duration should be determined at which similar structural effects are imposed by ETAF and an acceleration function representing the target hazard level. Regarding the ETAF generation method, the most rational selection for the representative ground motion is the average of records used in generation of ETAF. This selection respects the required similarity between the ETAF and the representing ground motions. It is also well consistent with the ET method's objective to replace the base records with the generated ETAF for predicting seismic response of structures at different seismic hazard levels following design guidelines (e.g., ASCE 7-05 [7] and ASCE 41-06 [1]). These standards allow the structural response to be determined by averaging the responses obtained from a suit of seven ground motions.

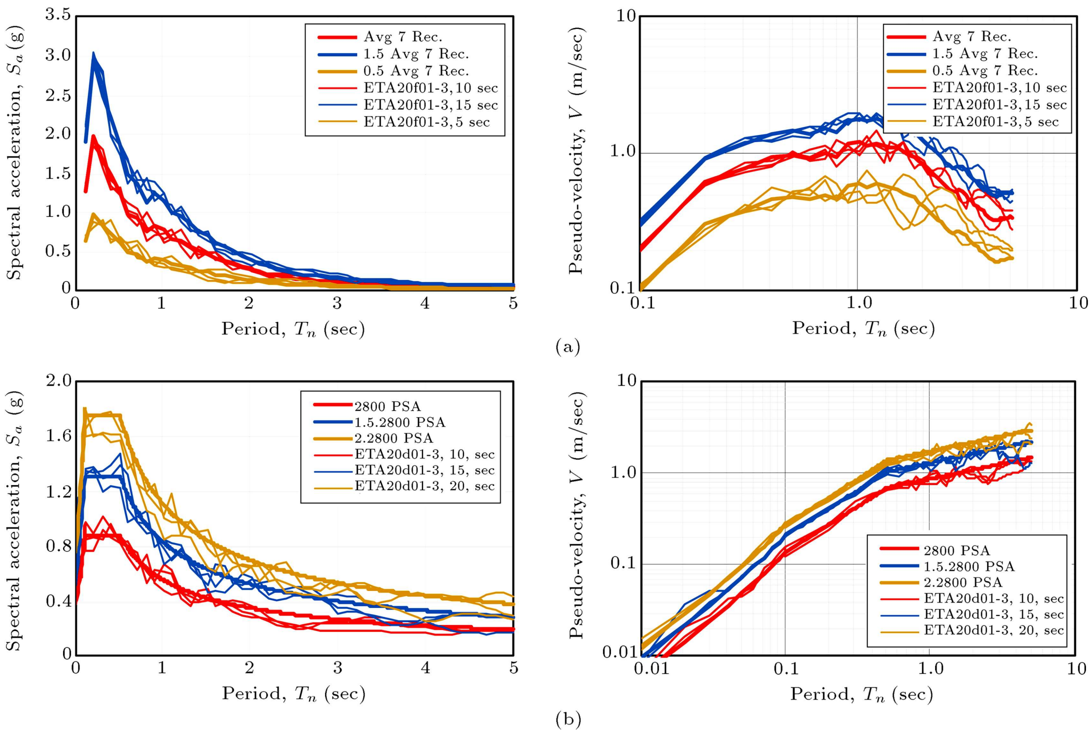


**Figure 2.** Comparison of the spectral acceleration and pseudo-velocity spectra related to ETAFs generated using (a) averaged spectrum from a suit of ground motion accelerations and (b) the design code acceleration spectrum in three seismic hazard levels.

## 2. Equivalent target time

Based on the characteristics of ETAF, the spectral acceleration corresponding to an analysis duration equal to the base target time, $t_{eq0}$, matches that of the base spectrum. Also, it is known that multiplying the duration time by an A factor leads the spectral response acceleration to amplification by an "A" factor, too. Therefore, the endurance time equivalent to a desired earthquake mean return period, $P_R$ (corresponding to a target exceedance probability) and structural natural period, $T_n$, which is denoted by $t_{eq}(P_R, T_n)$, can be defined using Eq. (1):

$$t_{eq}(P_R, T_n) = \tau(P_R, T_n).t_{eq0}, \tag{1}$$

where $\tau(P_R, T_n)$ is the ratio between the spectrum with a return period equal to $P_R$ and the base spectrum at the structural natural period, $T_n$. Although the spectral acceleration of generated ETAFs well matches the target spectrum by setting ETAF duration equal to $t_{eq0}$, a matching between the generated ETAFs and the base accelerograms has not been achieved, at the generation time, for other ground motion characteristics. To check if the consistency required for the purpose of this study exists between ETAFs and the base acceleration records, an initial evaluation is performed on the base target time. This evaluation and the criteria considered for it are the subject of the following section.

## 3. Evaluation of base target time

As previously stated, the "e", "f", and "h" ETAFs have been developed based on an spectrum averaged from seven scaled accelerograms. Therefore, the criterion considered for evaluating the appropriateness of the base target time has been adequate in matching ETAFs with the underlying accelerograms regarding spectral magnitude. The main characteristics of the ETAFs in representing the strong-motions can be named as amplitude, frequency content, and duration. One or more of these parameters have been used by previous researchers to represent ground motion characteristics [8,9]. The first factor, namely, amplitude, has already been considered in terms of spectral acceleration in natural period of structure when generation of ETAFs is undergone [10]. The fitting between the spectral amplitude of the ETAFs and the underlying acceleration functions is shown in Figure 2.

For considering the frequency content and duration parameters, selection of proper Intensity Measurers (IM) is required. A list of potential IMs for such purpose can be found in studies performed by [11-13]. For the purpose of this paper, the utilized parameters include: strong motion duration, Arias Intensity (AI), and Root Mean Square of Accelerations ($a_{\text{rms}}$) [9].

It must be noted that, since the generated ETAFs match the base spectrum by using a base target time equal to 10 sec, changing this value to $t_{eq0}$ will require the ETAFs to be scaled by a $10/t_{eq0}$ factor so that the matching between the ETAFs and the base spectrum at the base target time can be maintained.

For evaluating the appropriateness of two typical candidates for $t_{eq0}$, namely, the 10 and 20 sec values, the obtained matching between the ETAFs and the average of underlying accelerograms is presented in the following sections. This has been done for the two IM parameters mentioned before.

### *3.1. Strong motion duration*

Several studies have proved the critical contribution of earthquake duration to the damages observed in foundation material as well as the structure [14-16]. For instance, Bertero [17] used experimental studies to prove that the structural systems and members were subjected to nonlinear cyclic deformation collapse due to damage accumulation, which is a result of strong motion continuation [18] and the persistence of $P - \Delta$ effects [19]. Therefore, earthquake duration plays an important role in increasing the destructive effect of an earthquake and the more the number of loading cycles, the more will be the cumulative damage. Providing a comprehensive definition of duration is only possible through considering, at least, the magnitude, attenuation, and site class parameters. In a review of 30 different definitions proposed for duration, Bommer and Martinez-Pereira [20] found that each of these definitions had their own pros and cons and resulted in a varied range of results. Based on their observations, they proposed a new definition for duration (see [19] for details). Figure 3 compares different definitions of the strong motion duration for a typical accelerogram.

Some preliminary studies on the relation between earthquake accelerogram's duration and the duration

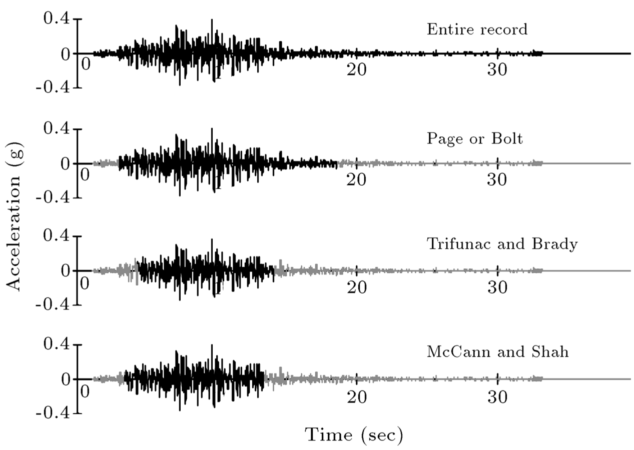


**Figure 3.** Comparison of strong motion durations of component LPLOB090 of Loma Pireta (No. 14 in Table 1).

**Table 1.** Specification of earthquake records.

| No | Date | Earthquake name | Record name | Magnitude (Ms) | Station number | PGA (g) | Scale factor |
|---|---|---|---|---|---|---|---|
| 1 | 10/17/89 | Loma Prieta | LPAND270 | 7.1 | 1652 | 0.244 | 2.6092 |
| 2 | | | LPAND360 | | | 0.24 | |
| 3 | | | LPAND-UP | | | 0.151 | |
| 4 | 06/28/92 | Landers | LADSP000 | 7.5 | 12149 | 0.171 | 3.6378 |
| 5 | | | LADSP090 | | | 0.154 | |
| 6 | | | LADSP-UP | | | 0.167 | |
| 7 | 04/24/84 | Morgan Hill | MHG06090 | 6.1 | 57383 | 0.292 | 1.8362 |
| 8 | | | MHG06000 | | | 0.222 | |
| 9 | | | MHG06-UP | | | 0.405 | |
| 10 | 10/17/89 | Loma Prieta | LPGIL067 | 7.1 | 47006 | 0.36 | 2.2035 |
| 11 | | | LPGIL337 | | | 0.325 | |
| 12 | | | LPGIL-UP | | | 0.191 | |
| 13 | 10/17/89 | Loma Prieta | LPLOB000 | 7.1 | 58135 | 0.45 | 2.2886 |
| 14 | | | LPLOB090 | | | 0.395 | |
| 15 | | | LPLOB-UP | | | 0.367 | |
| 16 | 01/17/94 | Northridge | NRORR360 | 6.8 | 24278 | 0.514 | 1.0731 |
| 17 | | | NRORR090 | | | 0.568 | |
| 18 | | | NRORR-UP | | | 0.217 | |
| 19 | 10/17/89 | Loma Prieta | LPSTG000 | 7.1 | 58065 | 0.512 | 1.437 |
| 20 | | | LPSTG090 | | | 0.324 | |
| 21 | | | LPSTG-UP | | | 0.389 | |

of ETAFs have been done by Mashayekhi and Estekanchi [21]. In the present study, three common definitions for the strong motion duration, namely, "Page and Bolt" [22], "Trifunac and Brady' [14], and "McCann and Shah" [15] methods, are considered. The "Page and Bolt" definition delimits the time span by the first and last occurrences of a threshold acceleration (e.g. 0.05 g) (Figure 4(a)) while the "Trifunac and Brady" method defines $t_d$ (duration time) as the time at which the Arias intensity computed by Eq. (2) stops further sensible growth (Figure 4(b)):

$$I_A = (\pi/2g) \int_0^{t_d} [a_g(t)]^2 \, dt, \tag{2}$$

where $a_g(t)$ is the ground acceleration, $t_d$ is the evaluated duration of the record, and $g$ is the gravitational acceleration. The McCann and Shah [15] method is based on the averaged input energy and calculates the duration based on the root mean square of the acceleration, $a_{\mathrm{rms}}$ using Eq. (3):

$$a_{\mathrm{rms}} = \left\{ \frac{1}{T_2 - T_1} \int_{T_1}^{T_2} [a_g(t)]^2 dt \right\}^{1/2}, \tag{3}$$

where $T_1$ and $T_2$ are the start and the end times of the record, respectively. $T_2$ was proposed by McCann and Shah [15] to be selected as the time in which the derivative of $a_{\mathrm{rms}}$ became negative and did not change sign unto the end of record. A similar criterion was proposed for selection of the start time, $T_1$, as the time in which the derivative changed sign for the first time after the record initiation [15] (Figure 4(c)).

Based on the above three methods, strong motion duration has been calculated for the 21 records listed in Table 2 and the results are presented in Figure 5. The mean strong motion durations computed using the first, second, and third methods are 14.6, 11.8, and 9.6 sec, respectively. Also, the mean strong motion durations for the first, second, and third methods of the ETAFs "e", "f", and "h" are 15.8 sec, 11.6 sec, and 9.5 sec, respectively.

### *3.2. Arias intensity*

In addition to the duration parameter considered in the previous section for assessing the appropriateness of different base target times, the Arias intensity is used in this section. This parameter is a representative of the energy demand spectrum of a strong motion and is used in this study as a characteristic of earthquake energy [16]. The Arias intensity is defined as the

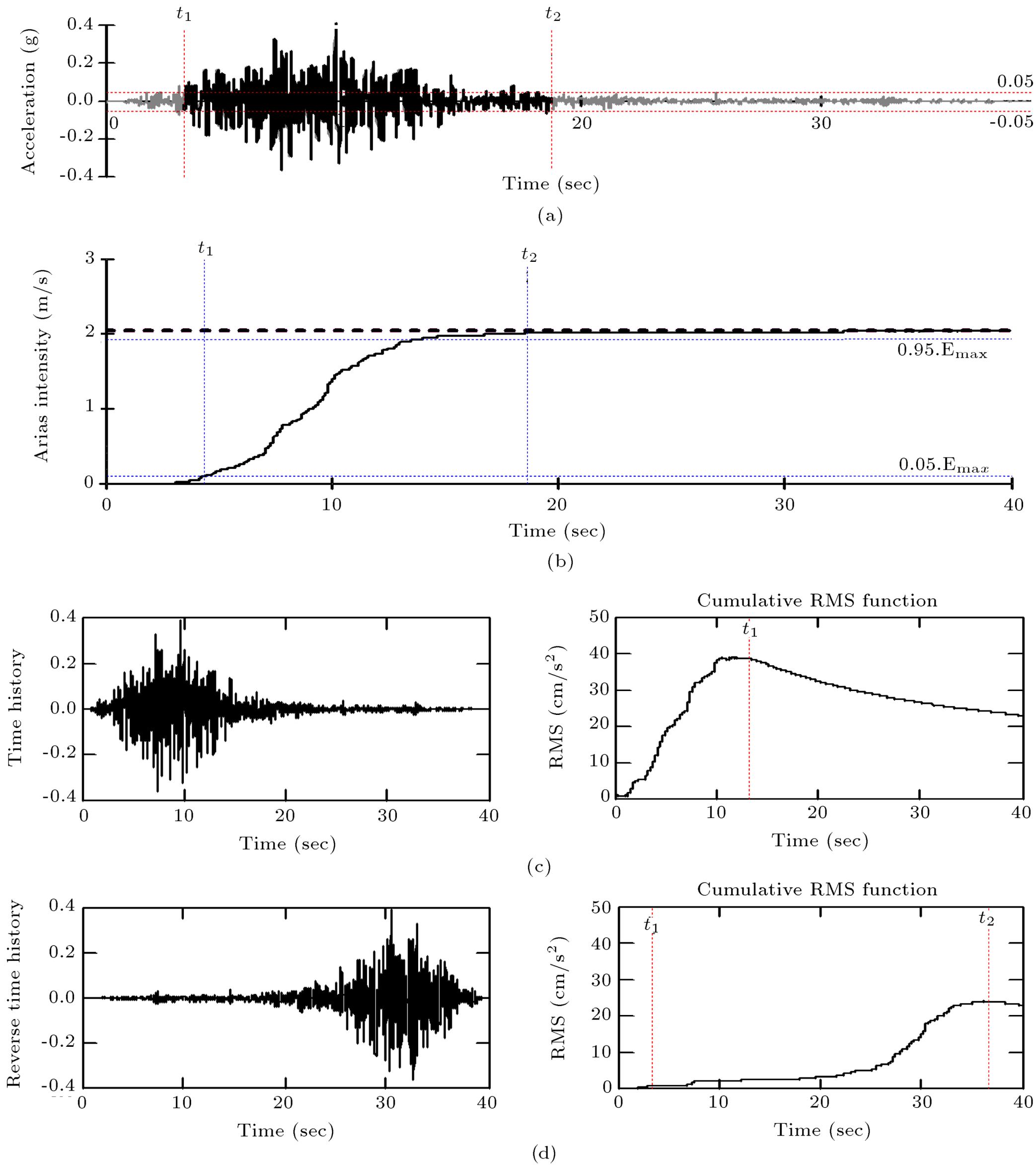


**Figure 4.** Specification of strong motion duration: (a) Page and Bolt, (b) Trifunac and Brady, and (c) McCann and Shah; for component LPLOB090 of Loma Pireta (Rec. No. 14, Table 1).

total kinetic energy induced on an elastic un-damped SDOF system and summated over a series of systems with different natural frequencies uniformly distributed from zero to infinity. This definition has been shown by Trifunac [14] and Arias [23] to lead to Eq. (2), previously presented.

For evaluating different candidates for base target time, the Arias intensity-time graphs are developed for seven earthquake records used for developing ETAFs after applying the scale factors shown in Table 1. The developed curves are shown in Figure 6(b).

Also, Arias intensities derived for six 20-sec ETAFs of types "e" and "f", and three 40-sec ETAFs of types "h" are shown in Figure 6(a). The Arias intensities calculated for each record before and after scaling are presented in Table 2 for different strong motion durations. To obtain a representative value according to which the validity of base target time can be assessed, the Arias intensities are averaged first for all the seven accelerograms and then for the proposed 4 strong motion durations. This has led to the 6.1 m/s value, which is presented in the ending part of Table 2 and can be considered for evaluating candidate base target times.

The averaged Arias intensities of ETAFs are illustrated in Figure 7 for candidate base target times of 10 and 20 sec. As previously stated, the acceleration intensities of the ETAFs were scaled by 0.5 in case of 20 sec target time to make them comparable to those with the 10 sec value. Comparing the results with the representative 6.1 m/s value (Figure 7(a)), $t_{eq0}$ = 10 sec is suggested as the most appropriate

**Table 2.** Seismic parameters for 7 accelerograms.

| Record | Comp.[a] | Met.[b] | $T_1$ (sec) | $T_2$ (sec) | $\Delta T$ (sec) | $\int a^2dt$ (m/sec) | $\int a^2dt$ (%) | $a_{\text{rms}}$ (cm/sec$^2$) | $\int a^2dt$ (m/sec) | $a_{\text{rms}}$ (cm/sec$^2$) |
|---|---|---|---|---|---|---|---|---|---|---|
| | | | | | | Not scaled records | | | Scaled records | |
| Loma Prieta 1989 | LPAND270 | A[c] | 0.00 | 39.61 | 39.61 | 0.797 | 100 | 14.18 | 5.42 | 37.00 |
| | | B[d] | 3.67 | 14.99 | 11.32 | 0.756 | 95 | 25.85 | 5.15 | 67.45 |
| | | C[e] | 4.31 | 14.82 | 10.51 | 0.717 | 90 | 26.11 | 4.88 | 68.13 |
| | | D[f] | 3.45 | 12.23 | 8.79 | 0.703 | 88 | 28.30 | 4.79 | 73.83 |
| Landers 1992 | LADSP000 | A | 0.00 | 50.00 | 50.00 | 0.707 | 100 | 11.89 | 9.35 | 43.25 |
| | | B | 3.44 | 37.58 | 34.14 | 0.658 | 93 | 13.88 | 8.71 | 50.50 |
| | | C | 6.30 | 38.10 | 31.80 | 0.636 | 90 | 14.14 | 8.41 | 51.44 |
| | | D | 5.48 | 31.04 | 25.56 | 0.582 | 82 | 15.09 | 7.70 | 54.88 |
| Morgan Hill 1984 | MHG06090 | A | 0.00 | 29.98 | 29.98 | 0.871 | 100 | 17.04 | 2.94 | 31.30 |
| | | B | 0.94 | 11.22 | 10.28 | 0.851 | 98 | 28.78 | 2.87 | 52.84 |
| | | C | 1.59 | 8.06 | 6.47 | 0.784 | 90 | 34.80 | 2.64 | 63.90 |
| | | D | 0.91 | 7.22 | 6.30 | 0.810 | 93 | 35.85 | 2.73 | 65.83 |
| Loma Prieta 1989 | LPGIL067 | A | 0.00 | 39.96 | 39.96 | 0.903 | 100 | 15.04 | 4.39 | 33.13 |
| | | B | 2.00 | 8.60 | 6.60 | 0.860 | 95 | 36.11 | 4.18 | 79.56 |
| | | C | 2.81 | 7.81 | 5.00 | 0.812 | 90 | 40.31 | 3.94 | 88.82 |
| | | D | 2.40 | 5.15 | 2.75 | 0.770 | 85 | 52.91 | 3.74 | 116.59 |
| Loma Prieta 1989 | LPLOB000 | A | 0.00 | 39.95 | 39.95 | 2.661 | 100 | 25.81 | 13.94 | 59.07 |
| | | B | 2.05 | 17.17 | 15.12 | 2.618 | 98 | 41.61 | 13.71 | 95.23 |
| | | C | 3.93 | 13.42 | 9.49 | 2.394 | 90 | 50.24 | 12.54 | 114.99 |
| | | D | 3.07 | 11.64 | 8.57 | 2.333 | 88 | 52.18 | 12.22 | 119.41 |
| Northridge 1994 | NRORR360 | A | 0.00 | 40.00 | 40.00 | 3.163 | 100 | 28.12 | 3.64 | 30.18 |
| | | B | 2.06 | 19.78 | 17.72 | 3.110 | 98 | 41.89 | 3.58 | 44.96 |
| | | C | 5.16 | 13.72 | 8.56 | 2.847 | 90 | 57.67 | 3.28 | 61.88 |
| | | D | 3.68 | 13.68 | 10.00 | 2.951 | 93 | 54.32 | 3.40 | 58.29 |
| Loma Prieta 1989 | LPSTG000 | A | 0.00 | 39.96 | 39.96 | 1.452 | 100 | 19.06 | 3.00 | 27.39 |
| | | B | 3.27 | 18.68 | 15.41 | 1.416 | 98 | 30.31 | 2.92 | 43.56 |
| | | C | 4.64 | 14.00 | 9.36 | 1.306 | 90 | 37.36 | 2.70 | 53.69 |
| | | D | 4.01 | 8.84 | 4.83 | 1.170 | 81 | 49.24 | 2.42 | 70.76 |
| Mean of records | | A | | | 39.92 | 1.508 | 100 | 18.73 | **6.10** | 37.33 |
| | | B | | | 15.80 | 1.467 | 96.429 | 31.20 | 5.87 | 62.01 |
| | | C | | | 11.60 | 1.356 | 90 | 37.23 | 5.49 | 71.84 |
| | | D | | | 9.54 | 1.331 | 87.143 | 41.13 | 5.28 | **79.94** |
| Mean of methods for mean of records | | | | | **12.31** | | | | **5.55** | **71.26** |

[a]Comp.: Component; [b]Met.: Method; [c]A: Entire record; [d]B: Page or Bolt; [e]C: Trifunac and Brady; and [f]D: McCann and Shah.

base target time regarding the Arias intensity parameter.

### 3.3. Root mean square of acceleration

Root Mean Square of Acceleration ($a_{\text{rms}}$) is an intensity measure used in seismology of strong motion and can be expressed using Eq. (3) [19]. This parameter reflects the effects of amplitude, frequency content, and duration, simultaneously [8]. For assessing the base target time, in this part, the $a_{\text{rms}}$ parameter is considered for evaluating the match between the generated ETAFs and the base records. $a_{\text{rms}}$ of the base earthquake

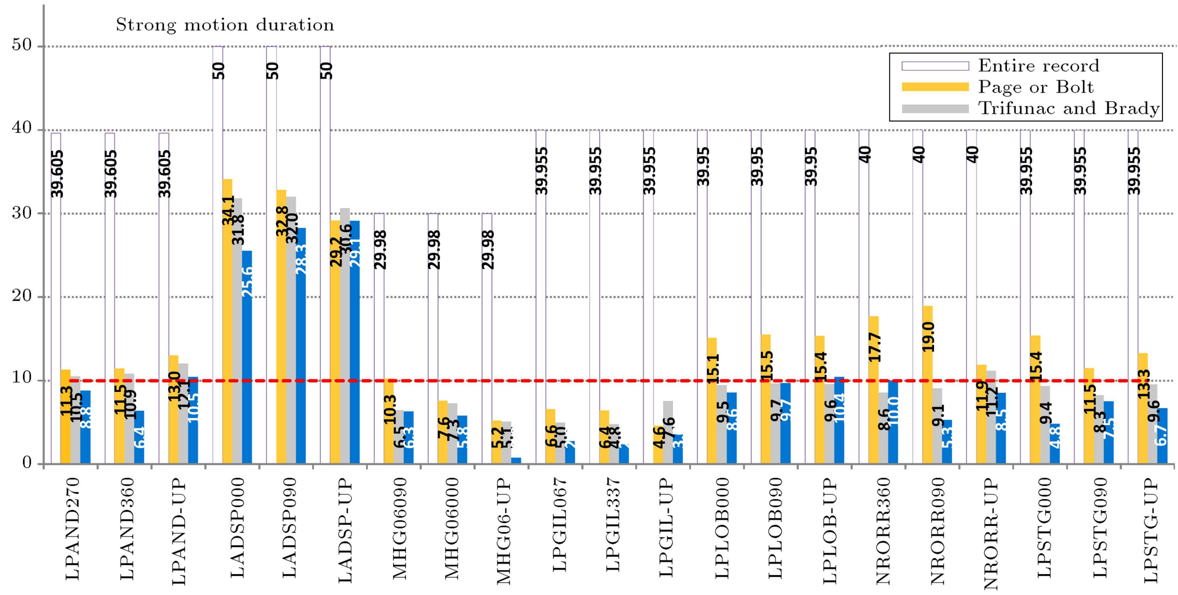


**Figure 5.** Strong motion duration for 21 records.

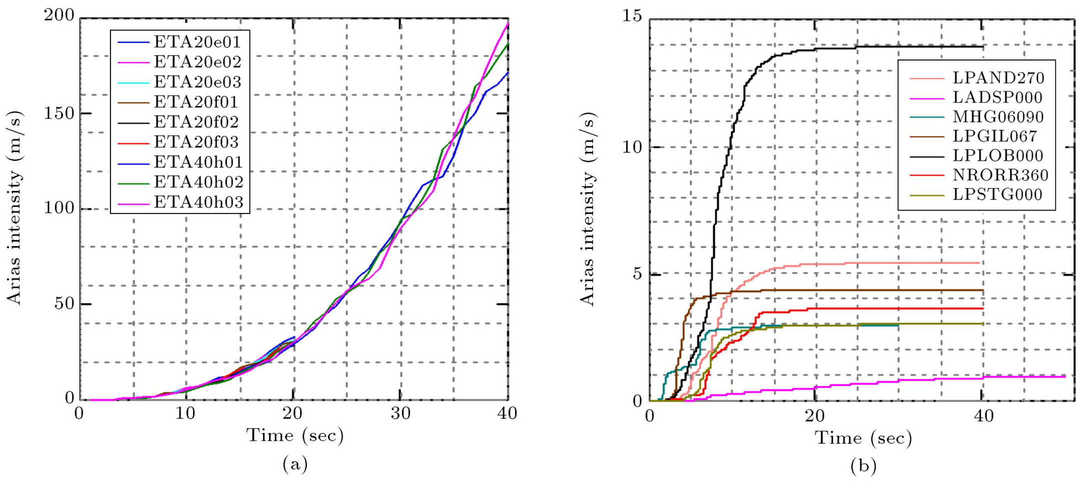


**Figure 6.** The Arias intensity for (a) 9 ETAFs and (b) seven accelerograms.

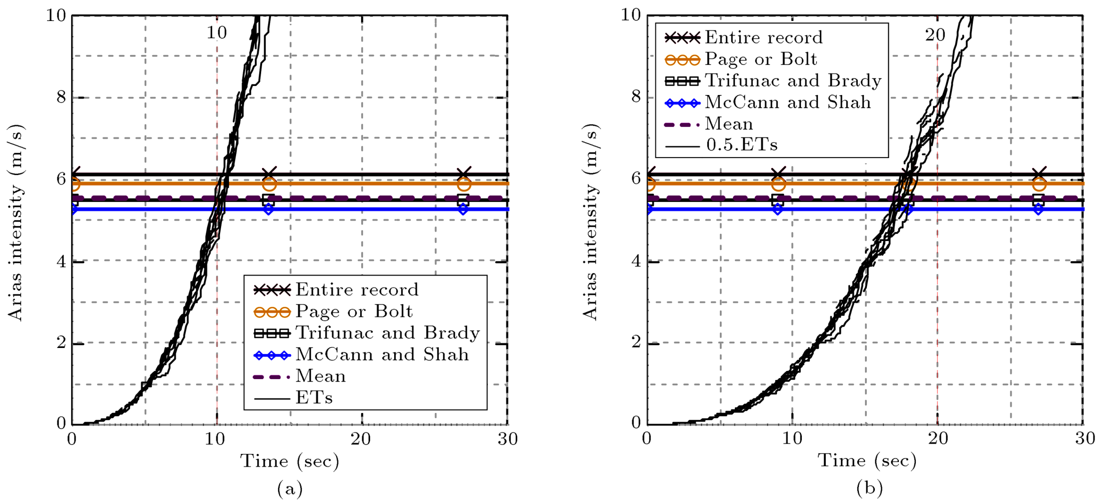


**Figure 7.** Comparison of the Arias intensity of the ETAFs and the accelerograms: (a) Proper matching of ETAFs in 10 sec and (b) Arias intensity of the ETAFs for target time of 20 sec.

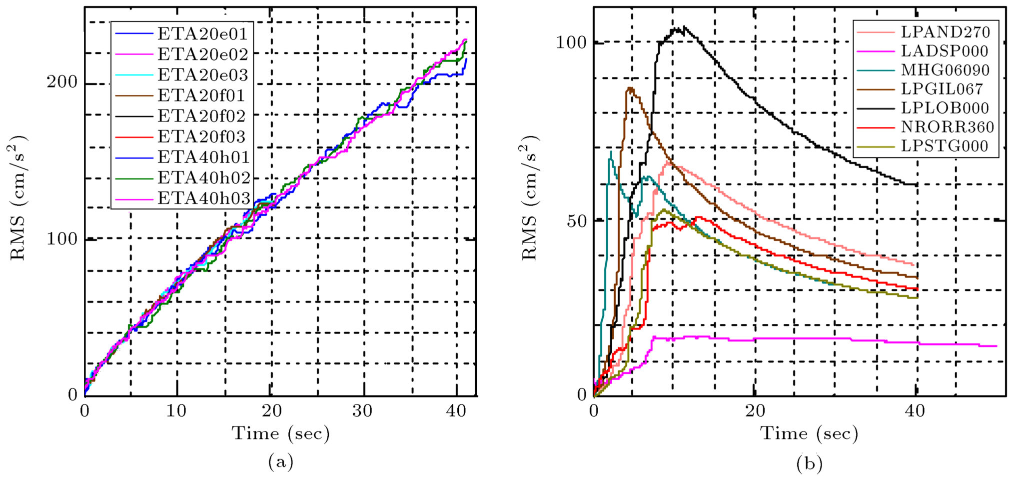


**Figure 8.** The root mean square of acceleration for (a) 9 ETAFs and (b) seven accelerograms.

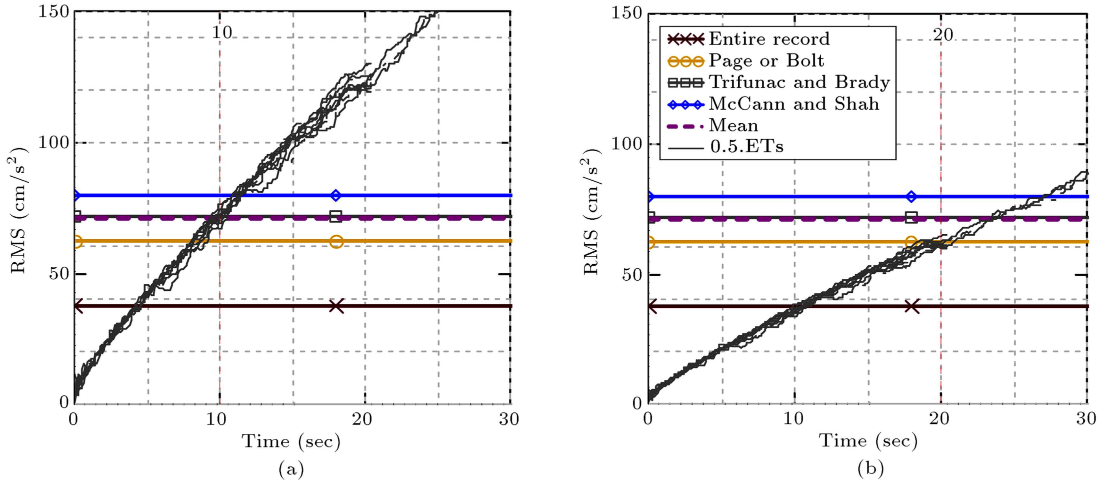


**Figure 9.** Comparison of $a_{\text{rms}}$ of the ETAFs and the accelerograms for (a) $t_{eq0} = 10$ sec and (b) $t_{eq0} = 20$ sec.

records is presented in Table 2 and illustrated in Figure 8(a) after applying the scale factors. Also, the values of $a_{\text{rms}}$ for six ETAFs previously used in Section 3.2 are shown in Figure 8(b).

The $a_{\text{rms}}$ values calculated for each record before and after scaling and using different duration definitions are presented in Table 2. Again, these values are summarized by averaging over all records and all duration values. The resulting 80 cm/sec$^2$ value is used for evaluating the $a_{\text{rms}}$ values of ETAFs, leading to suggestion of 10 sec as the proper base target time Figure 9(a). In Figure 9(b), the $a_{\text{rms}}$ values obtained using 20 sec target time (by scaling the values related to 10 sec target time by a 0.5 factor) are also compared with the results of the scaled accelerograms.

According to the evaluations performed using the three different seismological parameters in this section, $t_{eq0} = 10$ sec can be selected as the proper value for base target time. In the following sections, the spectral ratio, $\tau(P_R, T_n)$, is studied for various hazard levels regarding Eq. (1).

## 4. Spectral ratio

The spectral ratio denoted by $\tau(P_R, T_n)$ is the ratio of a spectrum with a return period equal to $P_R$ to the base target spectrum. This ratio can be derived for various structural periods, $T_n$. For calculation of this ratio, the response spectrum for each seismic hazard level should be first developed.

### *4.1. Development of response spectra for various return periods*

In order to develop response spectra for different return periods, the spectra and equations provided by ASCE41-06 [1] are adopted for Tehran City. In the following, the procedure used for deriving the equations and adapting them for Tehran City is described.

A study has been done by USGS on development of ground motion maps based on specified seismic risks. The 4-logarithmic curves developed for 2% and 5% probabilities of exceedance in 50 years are almost linear. On the other hand, in the regions denoted

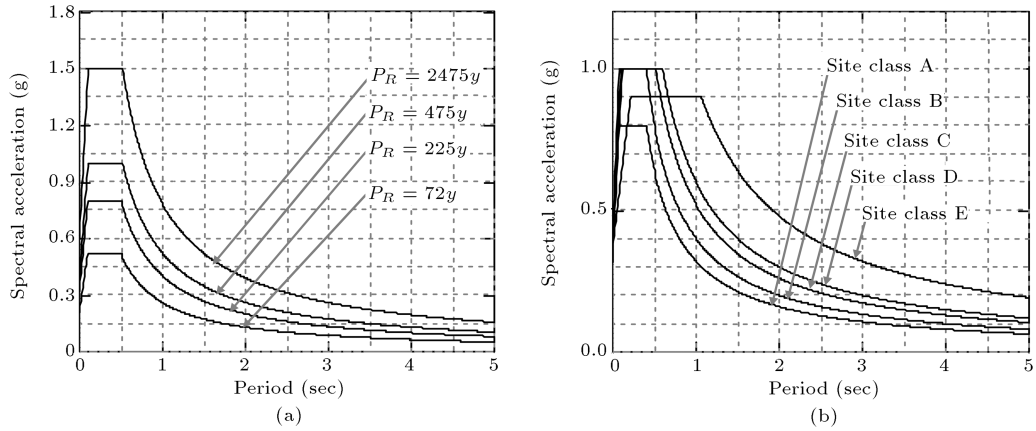


**Figure 10.** ASCE 41-06 acceleration spectra derived for (a) various seismic hazard levels in a site class C (using $S_S = 1.5$ and $S_1 = 0.6$) and (b) 10% probability in 50 years for all types of soil.

by the BSE-2 (Basic Safety Earthquake 2) map, the response spectrum with 2% exceedance probability in 50 years is directly used. Therefore, in these regions, an interpolation of the 4-logarithmic curve can be used for determination of acceleration response spectrum in arbitrary return periods falling in the 2% to 10% range of exceedance probability in 50 years. This approach is valid provided that the acceleration response spectrum in short periods, $S_S$, is less than 1.5. Eq. (4) (Eq. 1-1 of ASCE 41-06) [1] provides a closed-form solution to this logarithmic interpolation:

$$\ln(S_i) = \ln(S_{i10/50}) + [\ln(S_{iBSE-2}) - \ln(S_{i10/50})][0.606^* \ln(P_R) - 0.373], \quad (4)$$

where $\ln(S_i)$ is the natural logarithm of acceleration response spectrum ($i = S$ for short period and $= 1$ for the 1-sec period), $\ln(S_{iBSE-2})$ is the natural logarithm of acceleration response spectrum for 10% probability of exceedance in 50 years and in seismic hazard level BSE-2, and $\ln(P_R)$ is the natural logarithm of the desired mean return period corresponding to the probability of exceedance of a specific seismic hazard level. In regions where $S_S$ is equal to or greater than 1.5, the response spectrum contours on the response spectrum map are deterministic rather than probabilistic. In these regions, the values of response spectrum maps cannot be interpolated for calculation of the intermediate probabilities of exceedance. Instead, Eq. (5) (ASCE 41-06 Eq. 1-3) is used for assessing the acceleration response spectrum in arbitrary return periods by extrapolation from 10% probability of exceedance in 50 years by an approximate slope, which is defined by "$n$":

$$S_i = S_{i10/50}(P_R/475)^n. \quad (5)$$

This approximate slope of the seismic risk depends on the region. These values have been derived by USGS for California region, which is classified as the region with very high seismicity. A similar approach was used for derivation of the parameters of acceleration response spectrum with the probabilities of exceedance greater than 10% in 50 years in all regions [24]. In the region where USGS has no microzonation map, it is possible to use PGA and 2.5 PGA for approximating the acceleration response spectrum of long period ($S_L$) and short period ($S_S$), respectively [25]. Figure 10 depicts some examples of the generated spectra.

In order to assess the above equations and adapt them to Tehran City, the results of the study by Ghodrati et al. are used [20]. These results show that the PGA values vary from 0.27 g to 0.46 g for a 475 years return period, and from 0.27 g to 0.46 g for a 950 years return period. It must be noted that the Iranian seismic code "standard 2800" [26] postulates the 0.35 g PGA for 475 years return period. In a sum-up of these suggestions, the 0.4 g PGA is used as the base of calculations performed in this study. Figure 11 shows the seismic microzonation of Tehran and suburban areas in 475- and 950-year return periods (PGA on the bedrock), which has been generated by logic tree method (see [27]).

In order to derive the parameter "$n$" in Eq. (5) and evaluate the usability of Eq. (4) for Tehran City, the PGAs from these equations are drawn in Figure 12 against seismic hazard analysis results of Figure 11. The slope of the resulting graph suggests the "$n$" parameter to be taken as 0.24.

### *4.2. Different definitions of spectral ratio*

After developing the spectra for different seismic hazard levels, in the following, different definitions of spectral ratio ($\tau$) are presented. The value of target time corresponding to different hazard levels is then extracted using these alternative definitions for different soil conditions. The proposed alternative definitions

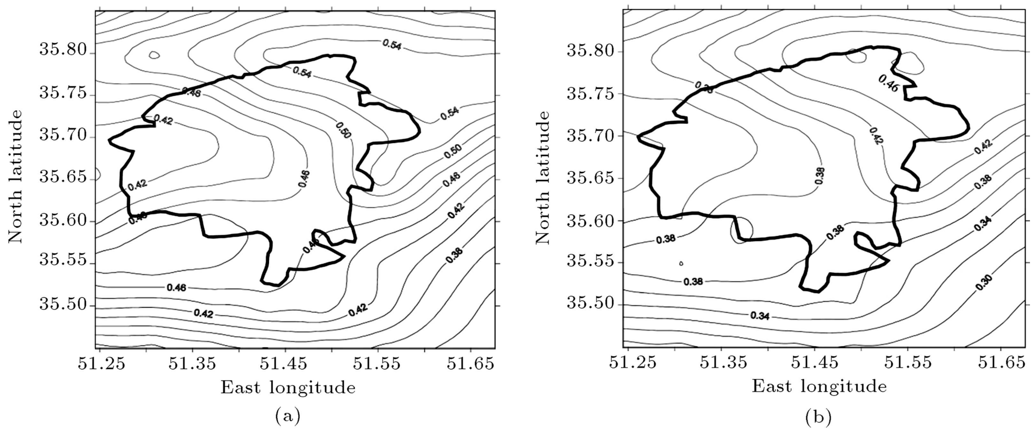


**Figure 11.** Seismic microzonation of Tehran and suburban areas by logic tree method (PGA on the bedrock): (a) 475 years return period and (b) 950 years return period. The solid line represents Tehran boarder (from [27]).

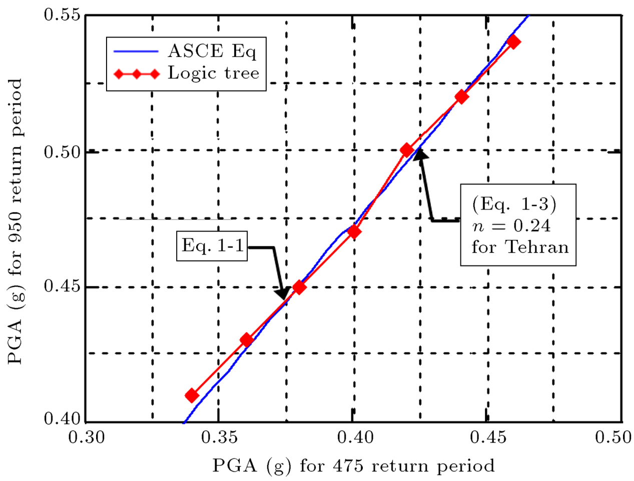


**Figure 12.** Comparison of the equations of two seismic hazard levels based on the equations adapted from ASCE 41-06 and the results of seismic hazard analysis using logic tree method and suggestion of the proper value for "$n$" parameter.

consider two different approaches for including structural period. The simpler "single-period" approach performs matching only at the structural period under consideration. The second more sophisticated "period-range" trend, which tries to account for higher mode effects and period elongation due to nonlinearity, performs matching at a period range starting from $\alpha_1 T_n$ and ending at $\alpha_2 T_n$, where $\alpha_1$ and $\alpha_2$ are constants and $T_n$ is the structural period. Utilizing a single period matching, the base spectrum can be considered either in its original form (obtained from averaging the base accelerogram spectra) or in the form of design code but scaled to the original spectrum. These two derivations of the single period matching form scaling methods "A1" and "A2".

Utilizing the "period-range" definitions, a number of methods are considerable for summarizing the relation between the target and base spectra observed at different points. The first method, denoted by "A3", averages the ratios obtained at different points. Mathematical presentation of this method in which summation has turned into integration can be expressed as Eq. (6):

$$\tau_3(P_R, T_n) = \int_{\alpha_1 T_n}^{\alpha_2 T_n} \frac{S_{a,P}(P_R, t)}{S_{a,T}(t)} dt. \qquad (6)$$

The second range summarizing method, identified by definition "A4", takes the maximum ratio obtained for the period range as the summarized value. The last range summarizing method, which is denoted by "A5" method, takes mean of absolute differences between the target and base spectra. A continuous form of this averaging will yield to an equation similar to Eq. (6) in which the division term is replaced by an "absolute of difference" term. The A1 to A5 definitions for the spectral ratio are summarized in Table 3.

**Table 3.** Summary of the spectral ratio definitions.

| Method name | Period treatment method | Base spectrum type | Period range summarization |
|---|---|---|---|
| A1 | Single-period | Averaged real spectrum | None |
| A2 | Single-period | Scaled code spectrum | None |
| A3 | Period range | Scaled code spectrum | Average of ratios |
| A4 | Period range | Scaled code spectrum | Maximum of ratios |
| A5 | Period range | Scaled code spectrum | Mean of absolute differences |

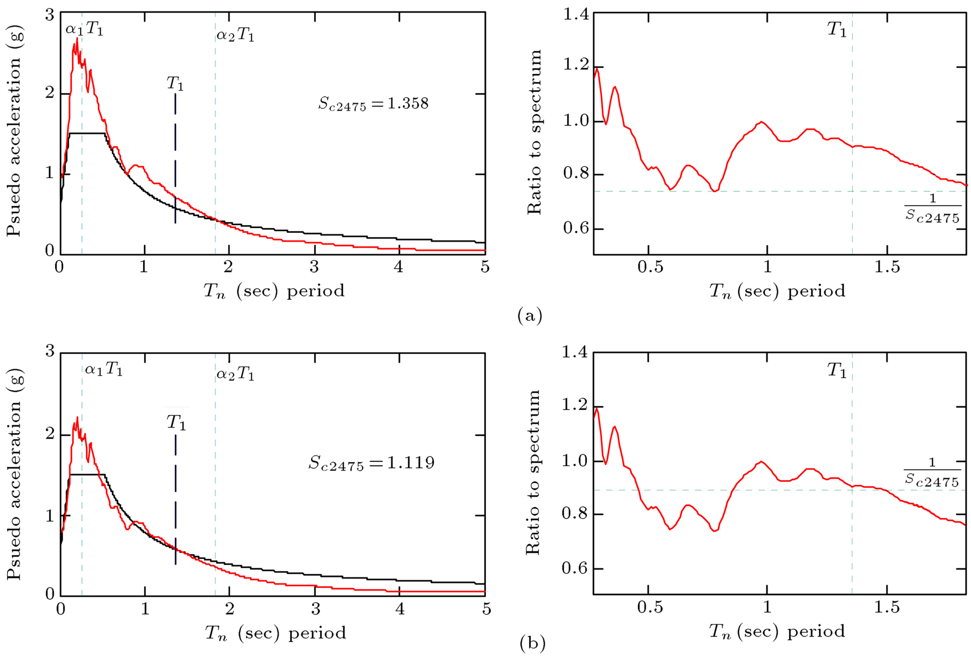


**Figure 13.** Scaling based on (a) "A4" and (b) averaging ("A3" or "A5") methods (see Table 3 for methods summary).

Typical scale values obtained from averaging methods "A3" and "A5" are compared with "A4" scaling values in Figure 13 for a building with the natural period of $T_n = 1.135$ sec using $\alpha_1 = 0.2$ and $\alpha_2 = 1.35$. In the right part of this figure, the ratio of the scaled spectrum to the code design spectrum in the natural period range is presented. The interesting fact is the perfect compatibility of the two spectra at the natural period of the building for averaging methods. This fact originates from selection of a proper prior scale factor for all accelerograms (presented in Table 1).

In all "A3" to "A5" methods, various values can be selected for $\alpha_1$ and $\alpha_2$ constants. In a code conforming manner, these parameters can be taken equal to 0.2 and 1.5 based on the ASCE 41-06 recommendation [1]. For enhanced consideration of different nonlinearities experienced by various structures having different linear and nonlinear period domains, these factors can be changed case by case. The values suggested by references [28,29] can be used for determining $\alpha_1$ and $\alpha_2$ parameters, respectively, for different structures.

Figure 14 shows the variation of the scale factor for various initiation and ending values of the period range. As can be seen, the scaling factor obtained using "A4" method following code suggestion (Figure 14(b)) for $\alpha_1$ greater than 1.35 dramatically increases and causes considerable difference between the two spectra, especially at the building natural period. As shown in Figure 14(a), the results obtained for averaging methods are not sensitive to the values used for the $\alpha_1$ and $\alpha_2$ parameters.

In Figure 15, results of all methods for target time are shown. As can be seen, the methods in which the period domain is used produce lower values of target time, suggesting that they would result in lower responses in structures.

According to the equations, it is observed that the target time for a specific seismic hazard level is a function of the natural period of buildings. Also, by variation of the target time for a specific seismic hazard level, considering changes in natural period of buildings is important, especially in utilization of "endurance time" method in structural evaluation before and after seismic rehabilitation where the natural period of the building is altered. For comparing the structural performance in the target time in different rehabilitation methods, the performance of the building should be studied at different target time points. Figure 16 shows variation of the target time with respect to natural period of the building for seismic hazard levels with return periods equal to 72, 225, 475, and 2475 years for various soil conditions. A structural engineer can determine target time of structures based on the main natural period of the structure under consideration.

According to the studies on the parameters of the ground motion strong duration, acceleration intensity, and root mean square of acceleration, it is concluded that 10 sec is the proper value for base target time $t_{eq0}$ in "endurance time" method and ETAF can lead to the same conditions up to this time when compared to the real accelerograms used in generation of ETAFs at the base seismic hazard in the main seismic parameters like strong motion duration, frequency content, and amplitude.

The target times in which the ETAFs' spectral

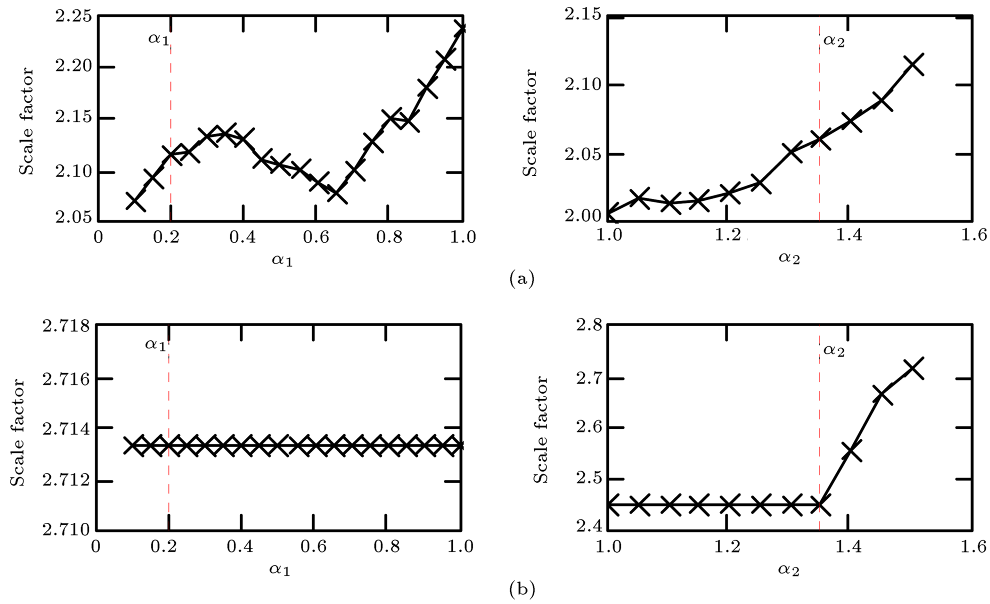


**Figure 14.** Variation of the scale factor for various initiation and ending natural period ranges: (a) Averaging method and (b) code method.

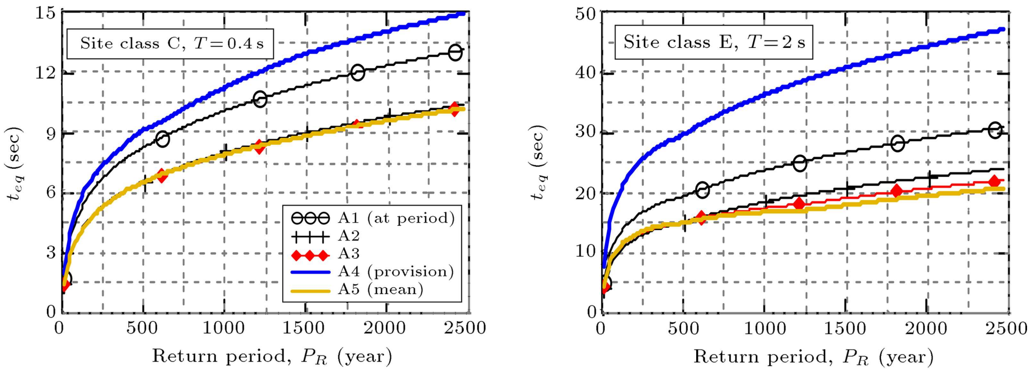


**Figure 15.** target time versus return period calculated based on definitions 1 to 5 (mentioned in Table 3) for various soils and for natural periods of the building equal to 0.4 sec and 2 sec (the acceleration parameters of the region are $S_S = 1.5$ and $S_1 = 0.6$).

amplitude coincides with different representations of the target spectra (explained in the previous section) are now specified. There still remains an essential question about the level of matching between ETAFs and the target spectra in terms of "duration" and "frequency content". For describing this essentiality, it must be noted that the direct relationship (increase in one with escalating the other) reported to exist between the amplitude and duration of natural ground motions also holds true for ETAFs. However, the "linear" relationship assumed in ETAF must be checked to determine if it describes the dominating natural earthquakes as well.

With a glimpse at the definition of the spectral ratio, it is obvious that the first definition is the most convenient method. This method, however, does not address the shorter periods (than the main period) corresponding to the higher vibration modes as well as the longer periods corresponding to softened system behavior. Still, it can be confidently used for seismic performance of an SDOF system in linear behavior range. The second, fourth, and fifth definitions yield the same results for the target time, except for soil type E (type IV according to Standard 2800 [26]) due to utilizing $Sc_m$ as an averaging scaling method. In this method, the effects of higher modes (lower natural periods) and structural nonlinearities (higher natural periods) are considered and these methods can be implemented for structures of any type in both linear and nonlinear phases. In fact, the second and the third methods in which code design spectrum pattern is used can be implemented for ETAF types "d" and "g", which are based on code spectrum. For types "d" and "g", the spectrum patterns of Iranian and ASCE7-05 [8] design codes are used, respectively, as the base spectrum for developing acceleration functions.

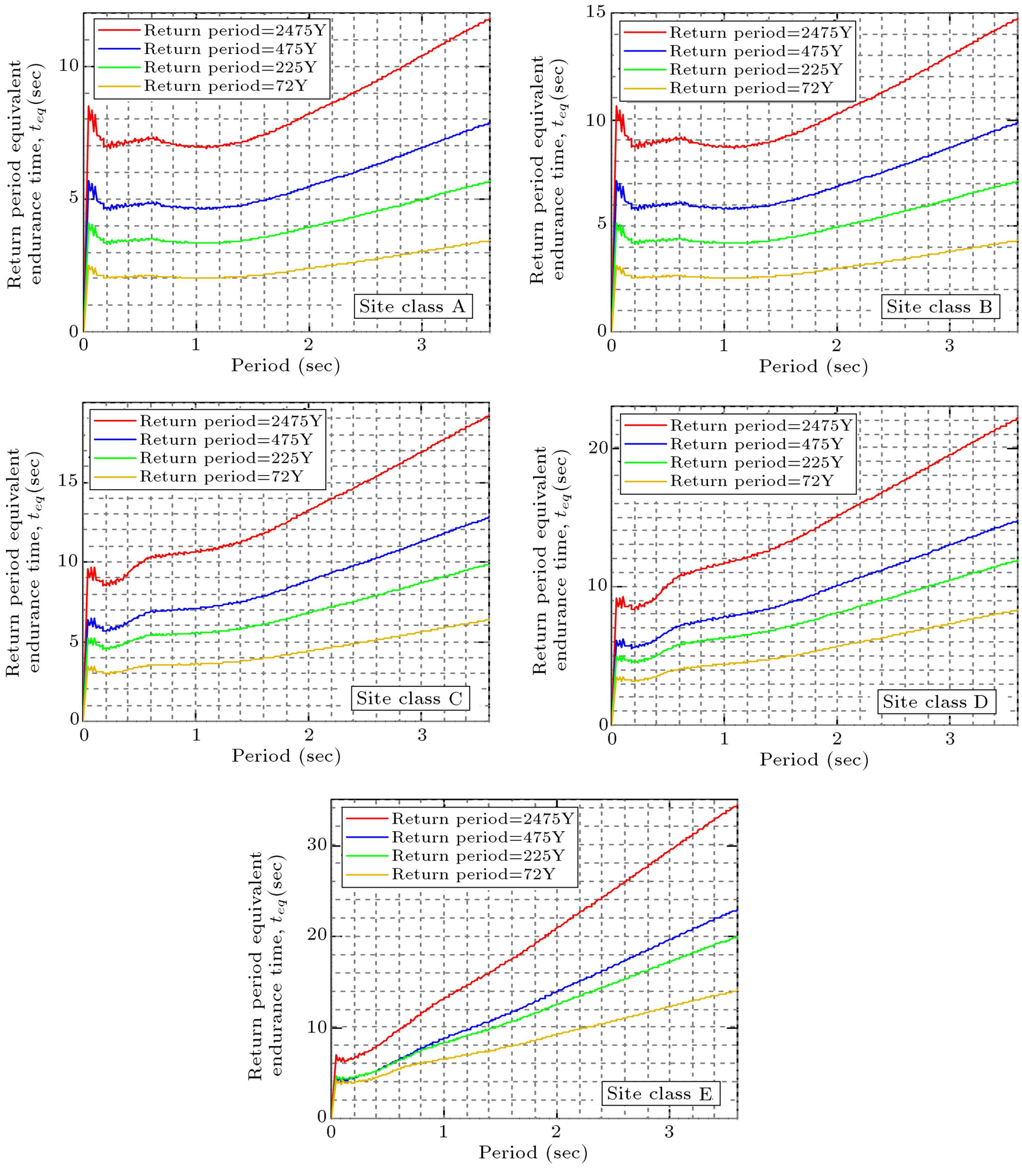


**Figure 16.** Target time versus natural period of building for seismic hazard levels with the return periods equal to 72, 225, 475, and 2475 years for various soil conditions based on the fifth method (the acceleration parameters of the region are $S_S = 1.5$ and $S_1 = 0.6$).

The fourth definition is the most compatible with the code definition, which results in the most conservative values for "endurance time" (largest value) and the fifth definition is closest to the results of the target spectrum. Thus, based on the structural type and desired reliability, each of the aforementioned definitions can be utilized.

After computation of the spectral ratio following either of the above definitions (A1 to A5), Eq. (7) can be used for determination of equivalent target times for various seismic hazard levels. In this equation, the matching of ETAFs to the target spectrum at the 10 sec duration is respected:

$$t_{eq}(P_R, T_n) = Sc_m(P_R, T_n).10 \text{ sec}. \quad (7)$$

## 5. Nonlinear structural analyses

In order to evaluate the reliability of ET analysis results and applicability of the proposed definitions in this study, Incremental Dynamic Analysis (IDA) is performed on the 30 Reinforced Concrete (RC) frames previously designed and studied by Haselton [30,31]. These frames cover a broad range of natural period (0.42 to 2.63 sec) and possess high ductility capacity and, therefore, can represent pre-collapse behavior. These frames have been modeled in Opensees software [32] by accounting for geometric ($P - \Delta$) and material nonlinearities. The latter has been reflected upon by using lumped plasticity method, in which the flexural hinges proposed by Haselton [30] are utilized.

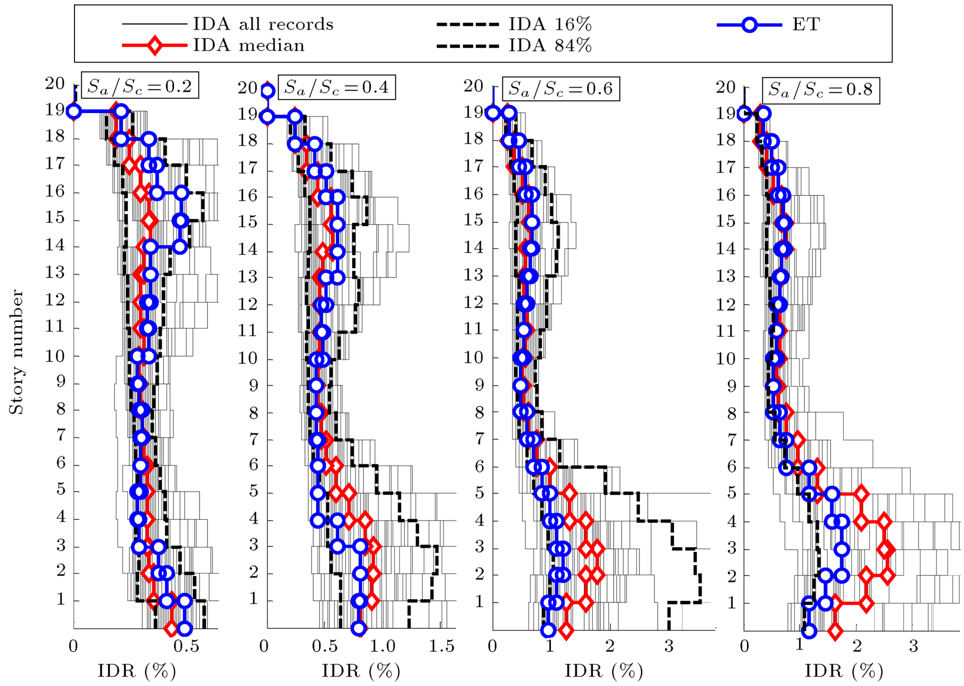


**Figure 17.** Interstory drifts estimated through IDA and ET at various intensity levels.

IDA analyses are performed using a set of 44 ground motion records recommended by FEMA P695 [33]. To compare the results of ET with those of IDA, the interstory drifts derived from ET method are compared with percentile (median, 16% and 84%) values estimated through IDA. This comparison is shown in Figure 17 for various $S_a/S_c$ levels. The $S_c$ parameter is the spectral acceleration corresponding to the collapse endurance time. Collapse endurance time is the ETAF time at which an analysis failure is observed due to excessive loss of strength in the structural model. Either of the A1 to A5 definitions of the spectral ratio (see Section 4.2 and Table 3) can be considered for establishing the correspondence between $S_c$ and collapse endurance times. In Figure 7, the A5 method has been used for extracting the $S_c$ values.

A quantitative comparison between the results can be performed by considering maximum interstory drifts (maximum among stories) as an overall response parameter and comparing the intensity values corresponding to various response levels. This is a response-based comparison in which the median intensity estimated by IDA is compared with the intensity denoted by ET method. To extract an overall index that reflects the ET error in complete range of responses, a summation is performed at multiple response levels using Eq. (8) to obtain the EDP error [34]:

$$\varepsilon_{\mathrm{EDP}} = \frac{1}{n_{(S_a=S_C)}} \sum_{i=1}^{n_{(S_a=S_C)}} \left| \frac{\mathrm{EDP}_{\mathrm{ET}} - \mathrm{EDP}_{\mathrm{IDA}}}{\mathrm{EDP}_{\mathrm{IDA}}} \right| \times 100(\%). \quad (8)$$

**Table 4.** Error values obtained for different structures and regarding various definitions of spectral ratio.

| No. of stories | Average $T_1$ (sec) | Spectral ratio definition | |
|---|---|---|---|
| | | A1 | A5 |
| 1 | 0.49 | 9.97 | 8.77 |
| 2 | 0.62 | 8.96 | 12.31 |
| 4 | 1.04 | 23.59 | 10.04 |
| 8 | 1.7 | 25.55 | 11.45 |
| 12 | 2.04 | 20.93 | 19.83 |
| 20 | 2.5 | 6.77 | 9.42 |
| Mean | | 18.45 | 13.07 |

Again, various spectral ratio definitions can be considered for extracting the $\mathrm{EDP}_{\mathrm{ET}}$ values and the corresponding error. Table 4 provides the $\varepsilon_{\mathrm{EDP}}$ errors corresponding to A1 and A5 definitions of spectral ratio and various structural heights. The A1 method is the simplest among all methods and the A5 is the one proposed by this article as the most accurate. It is also observed that the A5 scaling method benefits from the highest compatibility with the matching criterion used in generation of ETAFs.

## 6. Conclusion

In this study, based on the characteristics of the ETAFs, determination of target times associated with different seismic hazard levels is presented. Having established the endurance time-hazard level relationship, the structural response corresponding to a desired hazard level could be extracted by setting ETAFs duration equal to the related endurance time. Prior to establishing this relationship, the required matching between the available ETAFs and their underlying accelerograms was assessed in terms of different ground motion characteristics and the appropriateness of the base target time was verified. At the next stage, various alternatives were considered for reflecting upon ground motion intensity associated with a specific exceedance probability or return period. The "endurance time-return period" (i.e., the "intensity level-spectral ratio") correspondence was then established using various Intensity Measures (IMs). At the final part of this study, a set of 30 RC moment resisting frames were subjected to IDA analysis using 44 ground motion records and the median IM values corresponding to different structural response levels were extracted. These values were then compared with the ET-derived IMs regarding various definitions of IMs. The IM errors corresponding to various maximum interstory drift values were then computed and summated over the complete range of response levels to derive an overall error index. The error indices were then averaged for all structural models and compared for different IMs (spectral ratio definitions). This comparison revealed that the spectral ratio definition A5 led to the lowest errors due to the maximum compatibility it offered with the ETAF generation method.

## Nomenclature

| | |
|---|---|
| $A_{br}$ | Cross section area of brace |
| BRB | Buckling Restrained Bracing |
| BRBF | Buckling Restrained Braced Frame |
| BSO | Basic Safety Objectives |
| CP | Collapse Prevention |
| ET | Endurance Time |
| $I_O$ | Immediate occupancy |
| LS | Life Safety |
| NSP | Nonlinear Static Pushover analysis |
| NTH | Nonlinear Time History analysis |
| RHA | Response History Analysis |
| RP | Return Period |
| $S_1$ | Long-period response acceleration parameter |
| $S_a$ | Acceleration response spectrum of SDOF |
| $S_{ac}$ | Template acceleration response spectrum |
| $S_S$ | Short-period response acceleration parameter |
| $Sig$ | Standard deviation for a set of ground motions |
| TH | Time History analysis |
| $t_{eq}$ | Equivalent time in ET analysis |

## References


1. ASCE, *Seismic Rehabilitation of Existing Buildings*, ASCE 41-06, Reston, Virginia: American Society of Civil Engineers (2007).
2. Estekanchi, H.E. and Basim, M.C. "Optimal damper placement in steel frames by the endurance time method", *The Structural Design of Tall and Special Buildings*, **20**(5), pp. 612-630 (2011).
3. ASCE, *Minimum Design Loads for Buildings and Other Structures*, ASCE 7-10, Reston, Virginia: American Society of Civil Engineers, Structural Engineering Institute (2010).
4. Bazmooneh, A. "Application of endurance time method in seismic evaluation of existing steel buildings", M.S. Thesis, Sharif University of Technology, Tehran, Iran (2008).
5. Bazmooneh, A. "Probabilistic seismic demand analysis using Endurance time method", PhD Thesis. Sharif University of Technology, Tehran, Iran (2017).
6. Riahi, H.T. and Estekanchi, H.E. "Seismic assessment of steel frames with the endurance time method", *Journal of Constructional Steel Research*, **66**(6), pp. 780-792 (2010).
7. ASCE, *Minimum Design Loads for Buildings and Other Structures*, ASCE 7-05, 1st Ed. Reston, Virginia: American Society of Civil Engineers (2006).
8. Tabeshpour, M., *Conceptual, Applied Interpretation of Code for Seismic Design of Buildings Against Earthquake*, Tehran, Iran: Ganj-e-Honar (2006).
9. Naeim, E.d.F, *The Seismic Design Handbook*. Boston, MA: Springer US (2001).
10. Estekanchi, H.E., Vafai, A. and Sadeghazar, M. "Endurance time method for seismic analysis and design of structures", *Scientia Iranica*, **11**(4), pp. 361-370 (2004).
11. Yang, D., Pan, J. and Li, G. "Non-structure-specific intensity measure parameters and characteristic period of near-fault ground motions", *Earthquake Engng. Struct. Dyn.* **38**(11), pp. 1257-1280 (2009).
12. Riddell, R. "On ground motion intensity indices", *Earthquake Spectra,* **23**(1), pp. 147-173 (2007).
13. Narasimhan, S., Wang, M. and Pandey, M. "Principal component analysis for predicting the response of nonlinear base-isolated buildings", *Earthquake Spectra*, **25**(1), pp. 93-115 (2009).
14. Trifunac, M.D. and Brady, A. "A study on the duration of strong earthquake ground motion", *Bulletin of the*

*Seismological Society of America*, **65**(3), pp. 581-626 (1975).

15. McCann Jr, M.W. and Shah, H.C. "Determining strong-motion duration of earthquakes", In *Bulletin of the Seismological Society of America*, **69**(4), pp. 1253 -1265 (1979).

16. Baker, J.W., *Trade-offs in Ground Motion Selection Techniques for Collapse Assessment of Structures, VEESD, Vienna Congress on Recent Advances in Earthquake Engineering and Structural Dynamics* (2013).

17. Bertero, V.V. "Strength and deformation capacities of buildings under extreme environments", *Structural Engineering and Structural Mechanics*, **53**(1), pp. 29-79 (1977).

18. Bozorgnia, Y. and Bertero, V. Eds., *Earthquake Engineering: From Engineering Seismology to Performance-Based Engineering*, Boca Raton, Fla., CRC Press, London (2004).

19. Dowrick, D.J., *Earthquake Risk Reduction*, 2nd ed., Hoboken, NJ: John Wiley (2003).

20. Bommer, J.J. and Martinez-Pereira, A. "The effective duration of earthquake strong motion", *Journal of Earthquake Engineering*, **3**(2), pp. 127-172 (1999).

21. Mashayekhi, M. and Estekanchi, H.E, *Investigation of Shaking Characteristics of ET Excitation Functions Using Effective Number of Cycles of Motion, in 15th WCEE, World Conference on Earthquake Engineering*, (2012).

22. Bolt, B.A., *Duration of strong ground motion, in 5th WCEE: World Conference on Earthquake Engineering*, Vancouver, B.C., Canada (1974).

23. Arias, A. "A measure of earthquake intensity", in *Seismic Design for Nuclear Power Plants*, pp. 438-483 (1970)

24. FEMA, *NEHRP Commentary on the Quidliqnes for the Seismic Rehabilitation of Buildings*, FEMA, 274. Washington DC (1997).

25. FEMA, NEHRP, *Recommended Provisions for New Buildings and Other Structures: Training and Instructional Materials*, FEMA, 451B, Handouts, Washington DC (2007).

26. BHRC: Building and Housing Research Center, *Iranian Code of Practice for Seismic Resistant Design of Buildings*, Publication PNS-253, 3rd Ed., 135 pp., (in Persian) (2005).

27. Ghodrati Amiri, G., Motamed, R. and Rabet Es-Haghi, H. "Seismic hazard assessment of metropolitan" Tehran, Iran, *Journal of Earthquake Engineering*, **7**(3), pp. 347-372 (2003).

28. Kadas, K., Yakut, A. and Kazaz, I. "Spectral ground motion intensity based on capacity and period elongation", *J. Struct. Eng.*, **137**(3), pp. 401-409 (2011).

29. NIST "Applicability of nonlinear multiple-degree-of-freedom modeling for design supporting documentation", NIST GCR 10-917-9: Prepared for the National Institute of Standards by the NEHRP Consultants Joint Venture (2011).

30. Haselton, C.B., Ed., *Evaluation of Ground Motion Selection and Modification Methods: Predicting Median Interstory Drift Response of Buildings*, Berkeley, California: Pacific Earthquake Engineering Research, University of California at Berkeley (2009).

31. Haselton, C.B. and Deierlein, G.G., *Assessing Seismic Collapse Safety of Modern Reinforced Concrete Moment-Frame Buildings*. Berkeley, California: Pacific Earthquake Engineering Research Center, University of California at Berkeley (2007).

32. McKenna, F., Fenves, G.L. and Scott, M.H. *OpenSees: An Object-Oriented Software for Earthquake Engineering Simulation*: Pacific Earthquake Engineering Research Center (PEERC) (2004).

33. FEMA, *Quantification of Building Seismic Performance Factors*, FEMA P695. Washington DC (2009).

34. Lee, L.H., Han, S.W. and Oh, Y.H. "Determination of ductility factor considering different hysteretic models", *Earthquake Engng. Struct. Dyn.*, **28**(9), pp. 957-977 (1999).

## Biographies

**Amirali Bazmooneh** was born in Iran in 1983. He received the BE degree in Civil Engineering and ME degree in Earthquake Engineering from Sharif University of Technology (SUT), Tehran, Iran, in 2006 and 2009, respectively. He is PhD candidate in Structural and Earthquake Engineering at SUT. His research interests lie in the general area of performance-based design and structural design, especially seismic risk identification and decision-making; hazard mitigation and resilient infrastructure systems; structural dynamics and earthquake engineering; seismic design consideration of parametric architectural design; building information modeling; and software development. He has been focusing on generating and evaluation of the endurance time method as a powerful and rapid seismic analysis method during this years. He has contributed to several research projects in country scale such as seismic evaluation and design of squat shear wall technique for the seismic rehabilitation of existing typical schools, funded by Iran State Organization of Schools Renovation (2009-2011); codification of "Guidelines for Seismic Design of Substation Buildings, Structures, and Equipment in Iran" for the Ministry of Energy of Iran, funded by Moshanir Power Engineering Consultants Electrical and Electronic Manufacturing Company working with the Ministry of Energy (2008-2009); and preparation of seismic design guidelines for school modernization and equipping of schools in the country, funded by Iran State Organization of Schools Renovation (2006-2008).

**Homayoon Estekanchi** is a Professor of Civil Engineering at Sharif University of Technology. He received his PhD degree in Civil Engineering from SUT in 1997 and has been a Faculty Member at SUT since then. He is a member of Iranian Construction Engineers Organization, ASCE, Iranian Inventors Association, and several other professional associations. His research interests include a broad area of topics in structural and earthquake engineering with a special focus on the design of tall buildings and industrial structures.